THE JOURNAL OF PHYSICAL CHEMISTRY Letters

LETTER

pubs.acs.org/JPCL

Catalytic Activity of Pd/Cu Random Alloy Nanoparticles for Oxygen Reduction

Wenjie Tang, Liang Zhang, and Graeme Henkelman*

Department of Chemistry and Biochemistry, The University of Texas at Austin, Austin, Texas 78712-0165, United States

ABSTRACT: Trends in oxygen reduction activity of Pd/Cu bimetallic random alloy nanoparticles are determined with calculations of oxygen binding for a range of compositions. A reduction in the average oxygen binding is found as Cu is added to Pd, indicating an increase in catalytic activity up to a peak at 1:1 Pd/Cu ratio. Calculations show that Cu reduces the Pd−O binding energy and Pd increases the Cu−O binding energy. These changes are understood in terms of charge transfer from Pd to Cu, lowering the d-band center of Pd and raising that of Cu. The peak in activity occurs because these two effects not equivalent. A greater overlap between the d-states of Pd and the adsorbed oxygen makes the reduction in binding at Pd more significant than the increase in binding at Cu. We present a simple model of the average binding energy that can generally predict activity trends in random alloys.

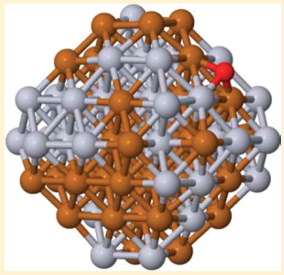

SECTION: Nanoparticles and Nanostructures

Alloying is a strategy that has been used to find non-Pt electrocatalysts that are effective and less expensive for the oxygen reduction reaction (ORR).[1−3] Mixing two or more metals can result in a catalyst that has distinct properties from its monometallic components. For example, it has been found that the addition of metals that bind oxygen strongly (Co, Ni, and Cu, etc.) can lower oxygen binding to more noble metals (Pt or Pd) and improve their ORR catalytic activity.[4−7] To aid the design of new alloy catalysts, calculations can be used to understand trends in activity and predict promising candidates for further investigation. The use of modern techniques to synthesize alloy nanoparticles with precise size and composition makes it easier to compare directly experiment with theory and better understand the relationship between the structure of nanoparticles and their catalytic function.[8]

The reduction of oxygen to water at a catalytic surface is a multistep reaction that includes at least two types of processes: O−O bond-breaking and the removal of the dissociation products by further reduction to H_2O. Whereas the overall reaction is complicated, it has been found that some simple reactivity descriptors can be used to predict activity trends across different catalysts. In the case of the ORR, Bligaard et al. have shown through the use of microkinetic models that the binding of oxygen (or hydroxyl) is an effective indicator of activity.[9] A reason that this simplification works is that for each elementary step in the reaction there is a Brønsted−Evans−Polanyi (BEP) correlation between the transition-state energy and the binding energy of the products.[10,11] Trends in oxygen binding are thus correlated to trends in transition-state energies for the dissociation of oxygen. In the weak binding regime, barriers are high and limit the overall kinetics. In the strong binding regime, the kinetics are limited by the removal of products from the catalysts. These two regimes can be seen in the so-called volcano plots where both weak and strong binding have low activity and the active catalysts, which provide a balance between these competing factors, are at the peak of the activity volcano. Using atomic oxygen binding as a reactivity descriptor for the ORR, a peak in activity is predicted at a binding strength slightly weaker than on the surface of bulk Pt.[12]

In this work, we investigate the effect of alloy composition in Pd/Cu nanoparticles on the ORR activity. Experimentally, Cu has been found to promote the activity of Pd at a ratio of 50%.[13,14] This enhancement in activity is intriguing because the binding of oxygen to Pd is stronger than optimal and the binding to Cu is stronger than both Pt and Pd. In a previous study, it was shown that Cu core−Pd shell particles have higher activity than monometallic Pd because subsurface Cu serves to weaken the binding of oxygen to the Pd surface, bringing it closer to the optimal.[15] The synergy between the two metals was understood in terms of an electronic interaction between subsurface Cu, which lowered the d-band center of the surface Pd and thus weakened the interaction with the oxygen adsorbate. In the case of random alloy particles, however, it is less clear how Cu could serve as a promoter, since Cu on the surface of the particle will bind oxygen more strongly than Pd. In this study, we calculate the binding of oxygen to random Pd/Cu alloys at different compositions and show that there is in fact weaker binding in the alloy than in pure Pd or Cu particles, which is consistent with the experimental observations. An analysis of the d-band center shows that the change in binding for the two metals is not the same, and this difference gives rise to the enhanced activity of the random alloys.

Calculations of oxygen adsorption on Pd/Cu random alloy nanoparticles were done with density functional theory (DFT) implemented in the VASP code.[16,17] The Kohn−Sham one-electron valence states were expanded in a basis of plane waves with a kinetic energy cutoff of 274 eV. The exchange-correlation energy was evaluated within the generalized gradient approximation with

Received: April 7, 2011
Accepted: May 16, 2011

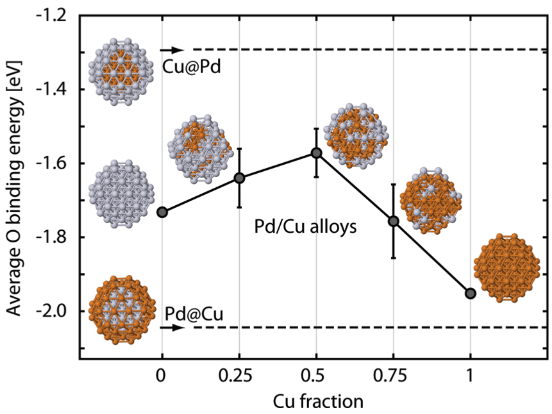

Figure 1. Average binding energy of oxygen on alloy Pd/Cu nanoparticles. Using this binding energy as a reactivity descriptor for the ORR indicates a peak in activity for random alloy particles at 1:1 compositions of Cu (dark color) and Pd (light color).

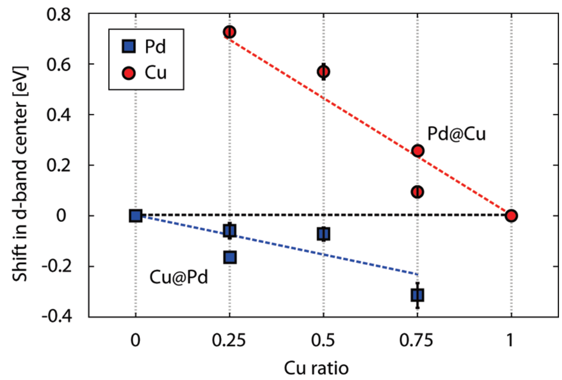

Figure 2. d-Band center shifts for Pd and Cu surface atoms in alloy particles with respect to the pure Pd and Cu particles, respectively. The d-band center of Pd is lowered by the addition of Cu, whereas the d-band center of Cu is raised by the addition of Pd.

the PW91 functional.[18] Core electrons were described by pseudopotentials with the projector augmented-wave (PAW) method.[19,20] Spin-polarization was tested and was used when necessary. A single Γ-point sampling of the Brillouin zone was used for the isolated particles. A vacuum gap of 8 Å separated the nanoparticles from their periodic images. All atoms in the nanoparticle were allowed to relax. Geometries were considered to be optimized when the force on each atom was <0.005 eV/Å.

Pd/Cu alloy nanoparticles were modeled as truncated octahedra containing 79 atoms. It is not known if this structure is the global minimum for each alloy particle, but it is the lowest energy structure that we found for a Pd nanoparticle of this size. As well as making the calculations simpler, keeping the same overall geometry allowed us to isolate the effects of varying the alloy composition. Random alloy particles with five different compositions were considered, varying in 25% increments. Particles with a 25%:75% ratio of component metals were considered in both random alloy and core–shell structures. A core–shell particle with 25% Cu, for example, has a core of 19 Cu atom and a shell of 60 Pd atoms and is denoted Cu@Pd. Random alloy geometries were constructed by randomly assigning each atom to the constituent metals, constrained to the specified overall composition. Ten configurations were generated for each random alloy composition. The binding of oxygen was calculated in the face-centered cubic (FCC) hollow site in the center of each of the eight (111) facets, giving a total of 80 binding energies in each average. The logic for focusing on the (111) facets is that these sites provide the weakest binding and, therefore, the highest activity for metals that bind oxygen stronger than Pt. Corner and edge sites bind oxygen more strongly and are assumed to be less active or poisoned during the reaction.

As part of our analysis to understand trends in binding energies, we use a Bader decomposition of the charge density into volumes around each atom.[21,22]

The average binding energy of atomic oxygen on Pd/Cu random alloy particles is shown in Figure 1. Because the binding of oxygen is an indicator of ORR activity, these data indicate that random alloy particles can have higher activity than those of pure Pd. The peak in activity is at a Pd/Cu ratio of 1:1, which is consistent with experiment.[13,14] The error bars show the standard deviation of the distribution of binding energies in the average over 80 sites. Whereas different local environments give rise to this distribution in binding energies, the trends over composition are significant. When the ratio of Cu is 75% and 100%, activity decreases to below that of Pd. The core–shell structures, Cu@Pd and Pd@Cu, fall beyond the extremes of the random alloy particles; Cu@Pd has the highest activity, whereas Pd@Cu has the lowest. It is interesting that the trend in oxygen binding for the random alloy particles is not linear between Pd and Cu. Even though Cu itself has a strong affinity for atomic oxygen, it weakens the binding in alloy particles. To determine the reasons for the activity enhancement in random alloys, we have studied in more detail how the addition of Cu affects the average binding of oxygen in Pd particles.

The origin of the average binding energy trends in the alloy nanoparticles can be understood by decomposing the interactions of oxygen with the individual metal types. Direct binding of oxygen to Cu is stronger than that to Pd. Hollow sites with three Cu atoms bind oxygen the strongest, on average, and those with three Pd atoms bind oxygen the weakest. Second neighbors also play a role; Cu atoms neighboring Pd decrease the Pd–O binding strength, and Pd atoms neighboring Cu increase Cu–O binding. These effects, however, are not symmetric because the average binding does not vary linearly as a function of composition between monometallic Cu and Pd particles. Particles with a 50% Cu/Pd composition bind oxygen significantly weaker than would be expected from a linear interpolation, as shown in Figure 1. The use of a d-band model to model separately the Pd–O and Cu–O interactions can help explain how the composition changes the average oxygen binding energy.

Hammer and Nøskov proposed a model in which the interaction between a metal surface and an adsorbate can be described as the interaction between the metal d-band and the adsorbate s or p orbitals.[23–25] When the change of the metal–O interaction, $\delta E_{\mathrm{metal-O}}$, is dominated by a shift in the d-band center position, $\delta\varepsilon_d$, a linear relationship arises

$$\delta E_{\mathrm{M-O}} \simeq -4 f_d \frac{V_{\mathrm{M-O}}^2}{|\varepsilon_d - \varepsilon_O|^2}\delta\varepsilon_d = \alpha_{\mathrm{M-O}}\delta\varepsilon_d \qquad (1)$$

where f_d is the local filling of the metal d states, ε_O is the center of the oxygen 2p states, and V^2 is the coupling matrix element between the oxygen orbitals and metal d-states. To a good approximation, changes in these values in alloys are smaller than changes in ε_d so to first-order in $\delta\varepsilon_d$, the binding of oxygen,

 dx.doi.org/10.1021/jz2004717 | J. Phys. Chem. Lett. 2011, 2, 1328–1331

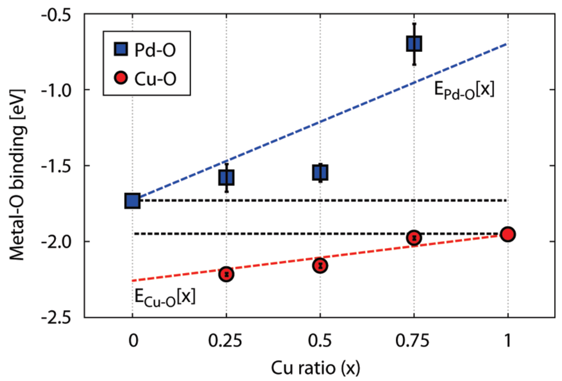

Figure 3. Pd−O binding (blue squares) and the Cu−O binding (red circles) from eq 1 for alloy particles with different ratios of Cu. The (dashed) trend lines are calculated from the linear fits in Figure 2 and eq 1. The Cu−O binding changes by a small amount, whereas the Pd−O binding is largely reduced by the addition of Cu.

E_{M-O}, varies linearly about ε_d.[25,26] We label the proportionality constant α_{M-O}.

To use this model to evaluate changes in oxygen binding due to alloying, we first need to quantify the change in the d-band level of surface atoms in the alloy particles. Figure 2 shows how the average d-band level of surface atoms change with respect to the pure metal particles. The lowering of the Pd d-band and the raising of the Cu d-band can be understood in terms of charge redistribution in the alloy. In the 50:50 Cu/Pd alloy, a Bader analysis shows that 0.15 e is transferred from Cu to Pd. For Pd, the d-type density of states at the Fermi level is 1.2 states/eV/atom so that the charge transfer lowers the d band with respect to the (increased) Fermi level by 0.125 eV. This d-band shift is consistent with the data in Figure 2.

To evaluate the effect of the d-band shifts on binding, we need to evaluate the constants α_{M-O} (M = Pd, Cu) from eq 1. These constants cannot be cleanly determined from the calculated energies of oxygen binding to the alloy particles because the contributions from the two metal types are not separable. It is this interaction between the metals that we would like to understand in terms of the d-band model. Instead of using the random alloy geometries, we use core−shell structures to determine α_{M-O} because there is a single metal type in the shell to which oxygen binds. Comparing a pure Pd particle to Cu@Pd shows a decrease in oxygen binding of 0.45 eV and a lowering of the surface Pd d band by 0.17 eV, yielding a slope α_{Pd-O} of −2.6. A fit of this correlation over a wider range of core metals gives a slope of −2.0.[15] Comparing Cu to Pd@Cu shows an increase in oxygen binding of 0.10 eV and an increase of the surface Cu d band of 0.26 eV, giving a slope α_{Cu-O} of −0.4.

The difference between α_{Pd-O} and α_{Cu-O} is central for understanding trends in oxygen binding to alloy particles. Whereas the magnitudes of charge transfer between the metal types and shifts in d-band centers are comparable, the larger magnitude of α_{Pd-O} as compared with α_{Cu-O} means that the change in oxygen binding energy will be larger for Pd than for Cu. The difference in magnitude can be understood in terms of the larger coupling matrix element (V^2_{M-O} in eq 1) between the oxygen adsorbate states and the metal d states in Pd as compared with Cu. The value of V^2 is estimated to be 2.8 times larger for Pd as for Cu, primarily because Pd is a larger element with diffuse d-electrons that overlap with the adsorbate states.[24,25]

Using our estimated values of α_{M-O} and eq 1, we can linearly transform the d-band data in Figure 2 to the binding energy data shown in Figure 3. Because $\alpha_{Pd-O} > \alpha_{Cu-O}$, there is a much larger change in the binding to Pd than to Cu as a result of alloying.

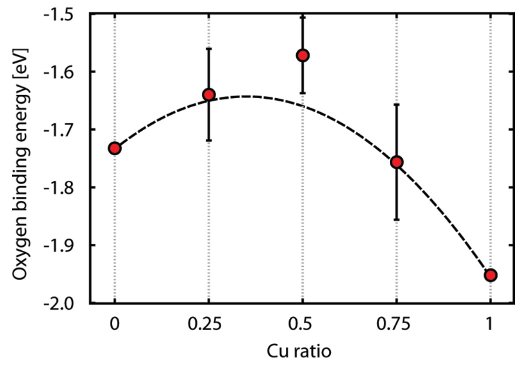

Figure 4. Comparison of the atomic oxygen binding energy calculated by DFT (red circle) and from eq 4 (dashed line).

The linear relationship between the oxygen binding energy and the component metals as a function of composition can be written as

$$E_{Pd-O}[x] = E^0_{Pd-O} + x m_{Pd-O} \qquad (2)$$

$$E_{Cu-O}[x] = E^0_{Cu-O} + (1-x) m_{Cu-O} \qquad (3)$$

where x is the composition of Cu, E^0_{M-O} is the binding to a pure particle of metal M, and m_{M-O} (M = Pd, Cu) are the slopes of the trend lines in Figure 3. The average binding to an alloy particle can then be written as a linear combination of these two functions, weighted by the composition of the component metals.

$$E_b[x] = (1-x)E_{Pd-O}[x] + xE_{Cu-O}[x] \qquad (4)$$

Expanding this gives

$$E_b[x] = (1-x)E^0_{Pd-O} + xE^0_{Cu-O} + (x-x^2)(m_{Pd-O} + m_{Cu-O}) \qquad (5)$$

where the first two terms are the linear interpolation between the binding at the pure metal particles, and the final term is a quadratic function that describes the relative change in binding due the metals' influence on each other. The values of m_{Pd-O} and m_{Cu-O} are of opposite sign because charge is transferred from Cu to Pd, and the shifts in d-band are in opposite directions. If the magnitudes of m_{Pd-O} and m_{Cu-O} were the same, then $E_b[x]$ would be a linear function; it is the difference in magnitude that gives rise to the nonlinear function and the peak in activity for the alloy.

The binding trend predicted by eq 4 fits the average binding energies calculated directly from DFT. (See Figure 4.) In the region of high Pd concentration, oxygen binding is largely determined by the Pd−O interaction, which becomes weaker as the Cu ratio increases. At high Cu concentrations, the binding is dominated by the strong Cu−O interaction. The weakest binding occurs at an intermediate Cu ratio,

$$x^* = \frac{1}{2} - \frac{E^0_{Pd-O} - E^0_{Cu-O}}{m_{Pd-O} - m_{Cu-O}} \qquad (6)$$

This composition is predicted by the model to be 40%, which is consistent to that found in our DFT binding calculations.

dx.doi.org/10.1021/jz2004717 |J. Phys. Chem. Lett. 2011, 2, 1328–1331

Activities of Pd/Cu random alloy particles are determined indirectly from the average binding energy of atomic oxygen on the (111) facets. Particles with 50% Cu are identified as the most active catalyst. The activity enhancement is due to a difference in how the two metals respond to a shift in their d-band centers. A charge transfer from Cu to Pd raises the d band of Cu and lowers that of Pd, resulting in a stronger oxygen binding to Cu and weaker oxygen binding to Pd. The change in Pd is much greater, however, because of stronger electronic coupling between Pd and the O adsorbate. We expect this to be a general description of adsorbate binding to random alloys, providing a prescription for tuning catalytic activity through alloying.

AUTHOR INFORMATION

Corresponding Author

*E-mail: henkelman@mail.utexas.edu.

ACKNOWLEDGMENT

This work was supported by the U.S. Department of Energy, Office of Basic Energy Sciences (grant DE-FG02-09ER16090) and the Robert A. Welch Foundation (grant F-160). Computing time was provided by the National Energy Research Scientific Computing Center and the Texas Advanced Computing Center at the University of Texas at Austin.

REFERENCES

(1) Shao, M. H.; Sasaki, K.; Adzic, R. Pd-Fe Nanoparticles as Electrocatalysts For Oxygen Reduction. *J. Am. Chem. Soc.* **2006**, *128*, 3526–3527.

(2) Shao, M. H.; Huang, T.; Liu, P.; Zhang, J.; Sasaki, K.; Vukmirovic, M. B.; Adzic, R. R. Palladium Monolayer and Palladium Alloy Electrocatalysts for Oxygen Reduction. *Langmuir* **2006**, *22*, 10409–10415.

(3) Ye, H.; Crooks, R. M. Effect of Elemental Composition of PtPd Bimetallic Nanoparticles Containing an Average of 180 Atoms on the Kinetics of the Electrochemical Oxygen Reduction Reaction. *J. Am. Chem. Soc.* **2007**, *129*, 3627–3633.

(4) Fernández, J. L.; Walsh, D. A.; Bard, A. J. Thermodynamic Guidelines for the Design of Bimetallic Catalysts for Oxygen Electroreduction and Rapid Screening by Scanning Electrochemical Microscopy. *J. Am. Chem. Soc.* **2005**, *127*, 357–365.

(5) Stamenkovic, V. R.; Fowler, B.; Mun, B. S.; Wang, G.; Ross, P. N.; Lucas, C. A.; Marković, N. M. Improved Oxygen Reduction Activity on Pt3Ni(111) Via Increased Surface Site Availability. *Science* **2007**, *315*, 493–497.

(6) Koh, S.; Strasser, P. Electrocatalysis on Bimetallic Surfaces: Modifying Catalytic Reactivity for Oxygen Reduction by Voltammetric Surface Dealloying. *J. Am. Chem. Soc.* **2007**, *129*, 12624–12625.

(7) Savadogo, O.; Lee, K.; Oishi, K.; Mitsushima, S.; Kamiya, N.; Ota, K.-I. New Palladium Alloys Catalyst for the Oxygen Reduction Reaction in an Acid Medium. *Electrochem. Commun.* **2004**, *6*, 105–109.

(8) Wilson, O. M.; Scott, R.W. J.; Garcia-Martinez, J. C.; Crooks, R. M. Synthesis, Characterization, and Structure-Selective Extraction of 1—3-nm Diameter AuAg Dendrimer-Encapsulated Bimetallic Nanoparticles. *J. Am. Chem. Soc.* **2005**, *127*, 1015–1024.

(9) Bligaard, T.; Nørskov, J. K.; Dahl, S.; Matthiesen, J.; Christensen, C. H.; Sehested, J. The Brønsted-Evans-Polanyi Relation and the Volcano Curve in Heterogeneous Catalysis. *J. Catal.* **2004**, *224*, 206–217.

(10) Brönsted, J. N. Acid and Basic Catalysis. *Chem. Rev.* **1928**, *5*, 231–338.

(11) Evans, M. G.; Polanyi, N. P. Inertia and Driving Force of Chemical Reactions. *Trans. Faraday Soc.* **1938**, *34*, 11.

(12) Nørskov, J. K.; Rossmeisl, J.; Logadottir, A.; Lindqvist, L.; Kitchin, J. R.; Bligaard, T.; Jónsson, H. Origin of the Overpotential for Oxygen Reduction at a Fuel-Cell Cathode. *J. Phys. Chem. B* **2004**, *108*, 17886–17892.

(13) Wang, X.; Kariuki, N.; Vaughey, J. T.; Goodpaster, J.; Kumar, R.; Myers, D. J. Bimetallic Pd-Cu Oxygen Reduction Electrocatalysts. *J. Electrochem. Soc.* **2008**, *155*, B602.B609.

(14) Fouda-Onana, F.; Bah, S.; Savadogo, O. Palladium-Copper Alloys as Catalysts for the Oxygen Reduction Reaction in an Acidic Media I: Correlation between the ORR Kinetic Parameters and Intrinsic Physical Properties of the Alloys. *J. Electroanal. Chem.* **2009**, *636*, 1–9.

(15) Tang, W.; Henkelman, G. Charge Redistribution in Core-Shell Nanoparticles to Promote Oxygen Reduction. *J. Chem. Phys.* **2009**, *130*, 194505.

(16) Kresse, G. Dissociation and Sticking of H2 on the Ni(111), (100), and (110) Substrate. *Phys. Rev. B* **2000**, *62*, 8295–8305.

(17) Kresse, G.; Hafner, J. First-Principles Study of the Adsorption of Atomic H on Ni (111), (100) and (110). *Surf. Sci.* **2000**, *459*, 287–302.

(18) Perdew, J. P.; Wang, Y. Accurate and Simple Analytic Representation of the Electron-Gas Correlation Energy. *Phys. Rev. B* **1992**, *45*, 13244–13249.

(19) Blöchl, P. E. Projector Augmented-Wave Method. *Phys. Rev. B* **1994**, *50*, 17953 .

(20) Kresse, G.; Joubert, D. From Ultrasoft Pseudopotentials to the Projector Augmented Wave Method. *Phys. Rev. B* **1999**, *59*, 1758.

(21) Bader, R. F. W. *Atoms in Molecules: A Quantum Theory*; Oxford University Press: New York, 1990.

(22) Tang, W.; Sanville, E.; Henkelman, G. A Grid-Based Bader Analysis Algorithm Without Lattice Bias. *J. Phys.: Condens. Matter* **2009**, *21*, 084204.

(23) Hammer, B.; Nørskov, J. K. Theoretical Surface Science and Catalysis - Calculations and Concepts. *Adv. Catal.* **2000**, *45*, 71–129.

(24) Hammer, B.; Nørskov, J. K. Electronic Factors Determining the Reactivity of Metal Surfaces. *Surf. Sci.* **1995**, *343*, 211–220.

(25) Ruban, A.; Hammer, B.; Stoltze, P.; Skriver, H. L.; Nørskov, J. K. Surface Electronic Structure and Reactivity of Transition and Noble Metals. *J. Mol. Catal. A* **1997**, *115*, 421–429.

(26) Xu, Y.; Ruban, A. V.; Mavrikakis, M. Adsorption and Dissociation of O2 on Pt-Co and Pt-Fe Alloys. *J. Am. Chem. Soc.* **2004**, *126*, 4717–4725.